Light Field Reconstruction Using Deep Convolutional Network on EPI (Supplementary Material)

Gaochang Wu, Mandan Zhao, Liangyong Wang, Qionghai Dai, Tianyou Chai, Yebin Liu

Abstract

This supplementary material provides more light field reconstruction results on microscopy light field data (Fig. 1), real-world scenes (Fig. 2) and synthetic scenes (Fig. 3). More depth enhancement results are demonstrated in this document (Fig. 4). We discuss the influence of reconstruction order on the reconstructed light field in Sec. 3. We present SSIM evaluations on each case in the paper in Sec. 4. In addition, we compare our framework with Zhang et al.*'s approach [37] on synthetic scenes in Table 5.*

1. Reconstruction Results

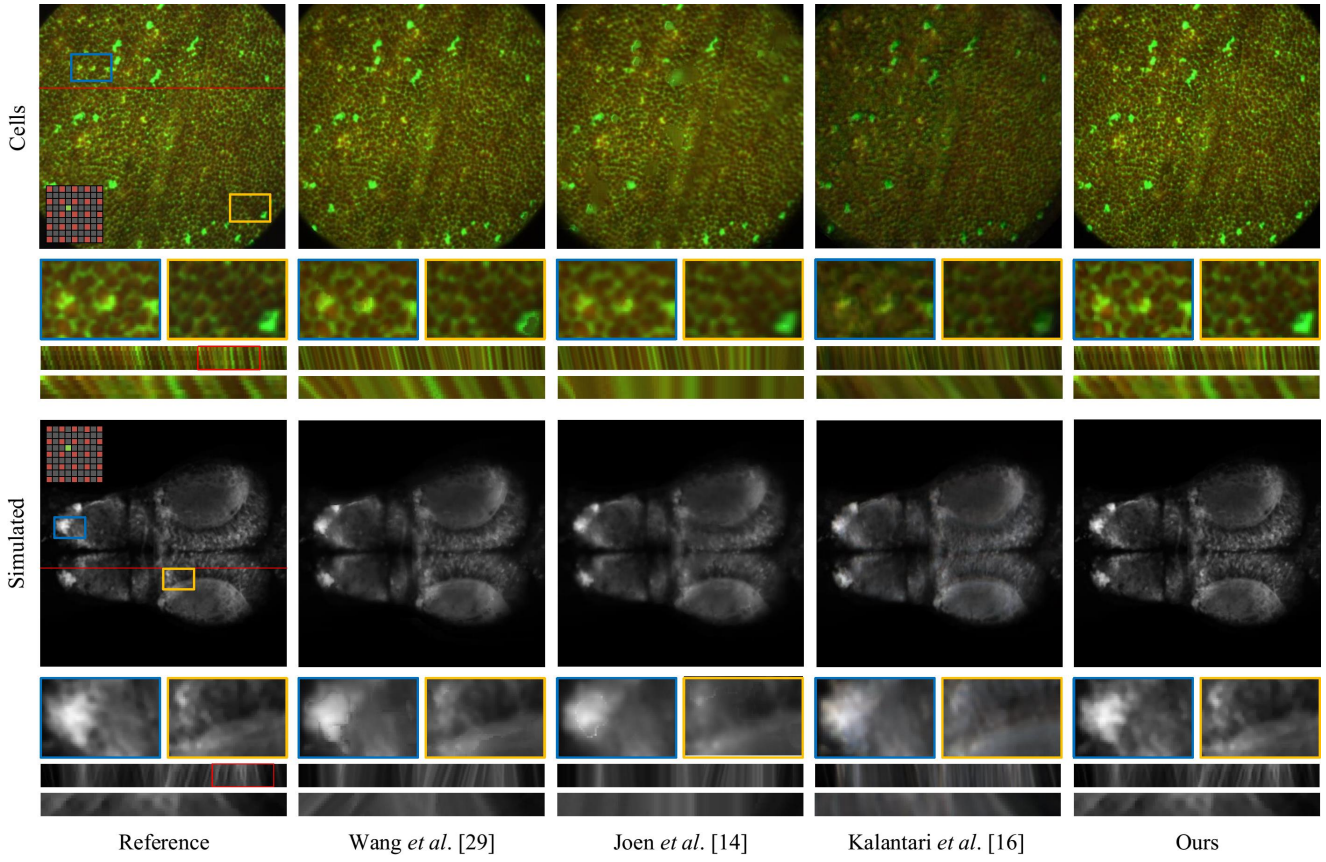

Figure 1. Comparison of light field reconstruction results on microscope light field datasets. The first row is provided by Lin *et al*. [23], and the second is a simulated microscope light field data

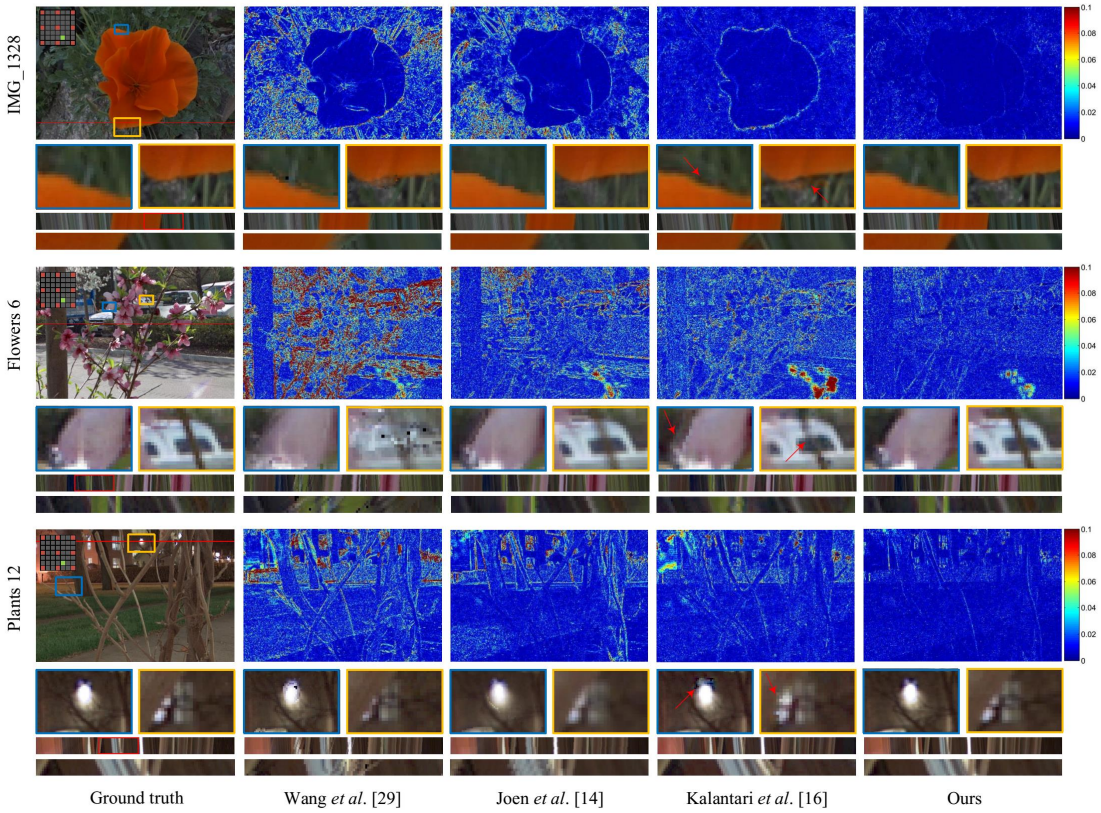

Figure 2. Comparison of light field reconstruction results on Lytro datasets (2). The first three rows are from Kalantari *et al.*'s dataset [29], and the others are from the Stanford Lytro Light Field Achieve [3]

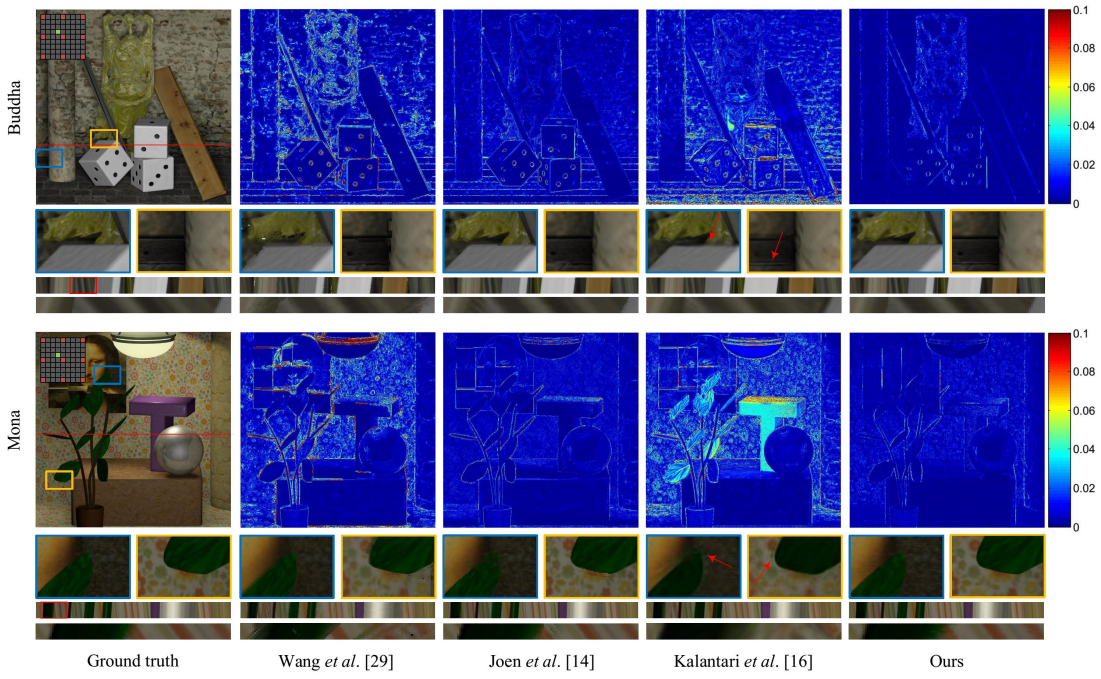

Figure 3. Comparison of light field reconstruction results on the HCI synthetic scenes [32].

2. Depth Enhancement Results

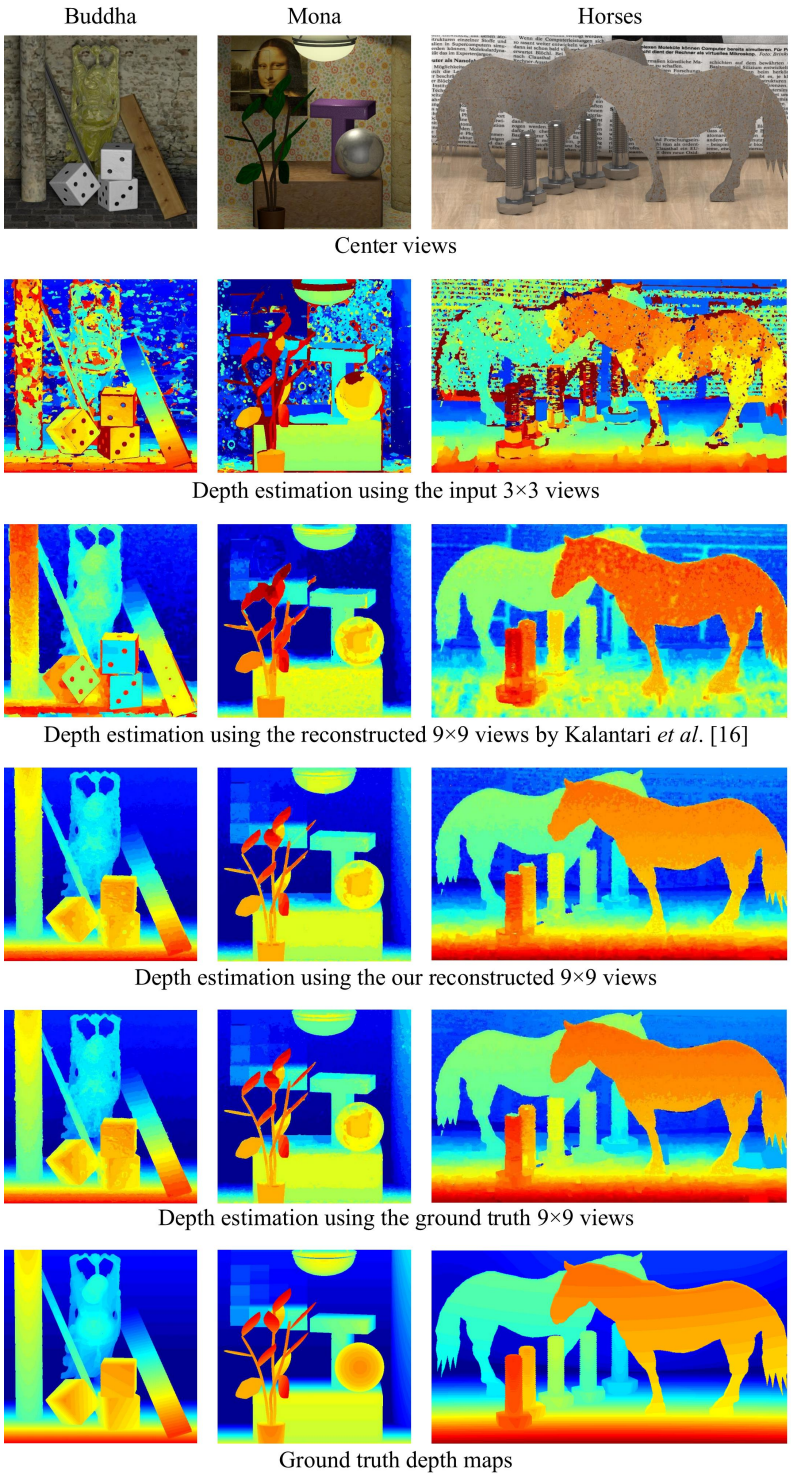

Figure 4. Depth estimation results using the approach by Wang *et al*. [29].

3. Reconstruction Order

In this section, we discuss the influence of order on the reconstructed light field. We describe the reconstruction for the full light field in Sec. 4.1. The input views shown in the red boxes in Fig. 5(a) are used to produce an intermediate light field (shown in Fig. 5(b)). To produce the final light field, images in the blue boxes in 5(b) can be used to generate novel views in the yellow box in Fig. 5(c). We refer this reconstruction order as *Order* 1. Alternatively, images in the green boxes in 5(b) can be also used to generate the novel views, and we refer this reconstruction order as *Order* 2. We compare these two reconstruction orders on synthetic scenes [32], and the numerical result is tabulated in Table 1. The two reconstruction orders influence very little on the final reconstructed light field, and we use *Order* 1 for all the other results.

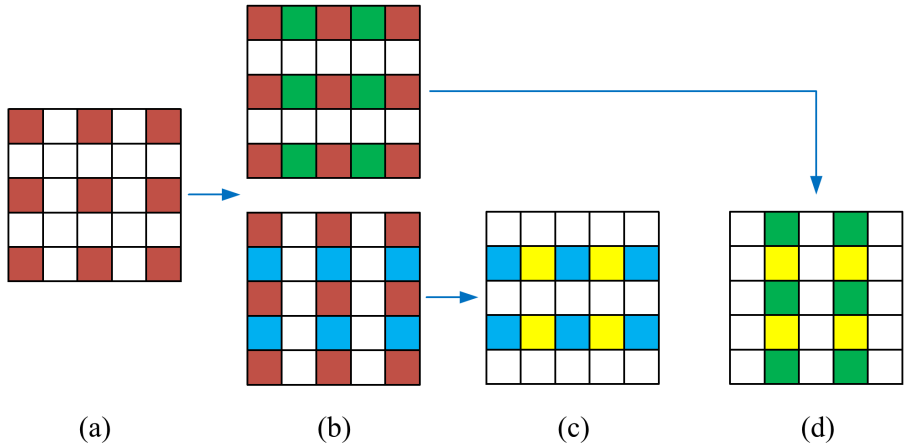

Figure 5. Reconstruction order of the full light field. (a) The input light field is composed by the images located at the red boxes; (b) The EPIs $E_{y^*,t^*}(x,s)$ are used to generate the novel views located at the green boxes, and the EPIs $E_{x^*,s^*}(y,t)$ are used to generate the novel views located at the blue boxes. (c) Images located at the blue boxes in (b) are used to generate the views located at the yellow boxes, and we refer this reconstruction order as *order* 1. (d) Alternatively, images located at the green boxes in (b) can be also used to generate the views located at the yellow boxes, and we refer this reconstruction order as *order* 2.

	Buddha	*Mona*
Order 1	46.42 / 0.9994	51.07 / 0.9996
Order 2	46.02 / 0.9992	50.96 / 0.9995

Table 1. Comparison of reconstruction orders on synthetic scenes [32] in terms of PSNR and SSIM.

4. Numerical Results

We provide SSIM evaluation in this section. Beyond that, we compare the proposed framework with Zhang *et al*. [37] on synthetic scenes using 3×3 input. Table 5 gives numerical result and the reconstructed light fields can be found in the video.

	30 scenes	*Reflective*29	*Occlusion*16
Wang *et al*. [29]	0.9071	0.8552	0.6977
Jeon *et al*. [14]	0.9289	0.9763	0.9348
Kalantari *et al*. [16]	0.9707	0.9541	0.9197
Ours/CNN only	0.9631	0.9902	0.9631
Our proposed	**0.9875**	**0.9929**	**0.9852**

Table 2. Quantitative results (SSIM) of reconstructed light fields on the real-world scenes. Corresponding to Table 1 in the paper.

	Neurons $20\times$	*Neurons* $40\times$
Wang *et al*. [29]	0.3881	0.4346
Jeon *et al*. [14]	0.7860	0.7583
Kalantari *et al*. [16]	0.6684	0.5551
Our proposed	**0.9378**	**0.9311**

Table 3. Quantitative results (SSIM) of reconstructed light fields on the microscope light field datasets. Corresponding to Table 2 in the paper.

	Buddha		*Mona*	
Input	3×3	5×5	3×3	5×5
Wang *et al*. [29]	0.9601	0.9987	0.9667	0.9989
Jeon *et al*. [14]	0.9959	0.9986	0.9969	0.9984
Kalantari *et al*. [16]	0.9728	0.9893	0.9633	0.9686
Ours/SC [34]	0.9975	0.9979	0.9973	0.9991
Ours/SRCNN [9]	0.9971	0.9981	0.9976	0.9989
Our proposed	**0.9980**	**0.9994**	**0.9982**	**0.9996**

Table 4. Quantitative results (SSIM) of reconstructed light fields on the synthetic scenes of the HCI datasets. The SC [34] and SRCNN [9] are applied to the proposed framework by replacing the residual learning method and are denoted as ours/SC and ours/SRCNN, respectively. Corresponding to Table 3 in the paper.

	Buddha	*Mona*
Zhang *et al*. [37]	38.13 / 0.9943	37.90 / 0.9947
Our proposed	**43.20 / 0.9980**	**44.37 / 0.9982**

Table 5. Comparison with Zhang *et al*. [37] on synthetic scenes using 3×3 input in terms of PSNR and SSIM.